Enhanced thermal stability of carbon nanotubes by plasma surface modification in Al_2O_3 composites

Hoonsung Cho,[1] Donglu Shi,[1,2,3,a)] Yan Guo,[1] Jie Lian,[4] Zhifeng Ren,[5] Bed Poudel,[5] Yi Song,[6] Jandro L. Abot,[6] Dileep Singh,[7] Jules Routbort,[8] Lumin Wang,[9] and Rodney C. Ewing[9]

[1]*Department of Chemical and Materials Engineering, University of Cincinnati, Cincinnati, Ohio 45221, USA*
[2]*The Institute for Advanced Materials & Nano Biomedicine, Tongji University Shanghai, 200092, China*
[3]*Institute of Micro/Nano Science & Technology, Shanghai Jiao Tong University, Shanghai 200240, China*
[4]*Department of Mechanical, Aerospace & Nuclear Engineering, Rensselaer Polytechnic Institute, Troy, NY 12180, USA*
[5]*Department of Physics, Boston College, Chestnut Hill, Massachusetts 02467, USA*
[6]*Department of Aerospace Engineering & Engineering Mechanics, University of Cincinnati, Cincinnati, Ohio 45221, USA*
[7]*Nuclear Engineering Division, Argonne National Laboratory, Argonne, Illinois 60439, USA*
[8]*Energy Systems Division, Argonne National Laboratory, Argonne, Illinois 60439, USA*
[9]*Departments of Geological Sciences, Nuclear Engineering & Radiological Sciences and Materials Science & Engineering, University of Michigan, Ann Arbor, Michigan 48109, USA*

(Received 28 May 2008; accepted 29 July 2008; published online 1 October 2008)

A plasma polymerization method was employed to deposit an ultrathin pyrrole film of 3 nm onto the surfaces of single wall carbon nanotubes (SWCNTs) and Al_2O_3 nanoparticles for developing high-strength nanocomposites. The surfaces of plasma coated SWCNTs and Al_2O_3 nanoparticles were studied by high resolution transmission electron microscopy (TEM) and time-of-flight secondary ion mass spectroscopy. After sintering the SWCNTs-Al_2O_3 composites at different temperatures (maximum of 1200 °C), the thermal stability of plasma-coated SWCNTs was significantly increased, compared to their uncoated counterparts. After hot-press sintering, the SWCNTs without plasma coating were essentially decomposed into amorphous clusters in the composites, leading to degraded mechanical properties. However, under the same sintering conditions, the plasma surface modified SWCNTs were well preserved and distributed in the composite matrices. The effects of plasma surface coating on the thermal stability of SWCNTs and mechanical behavior of the nanocomposites are discussed. © *2008 American Institute of Physics*. [DOI: 10.1063/1.2985915]

I. INTRODUCTION

The mechanical, thermal, and electrical properties of carbon nanotubes have prompted intense research into a wide range of applications in structural materials, electronics, chemical processing, and energy management.[1–3] For high-strength structural ceramics, Peigney *et al.*[4] developed an *in situ* growth of carbon nanotube/oxide nanocomposite powder technique. They fabricated composite ceramics from CNTs-Fe-Al_2O_3 nanocomposite powder via a hot-press sintering (HPS) process. The CNTs-Fe-Al_2O_3 powders were uniaxially hot pressed at 43 MPa in graphite dies, in a vacuum pressure, at 1500 °C with a dwell time of 15 min.[5–8] Although considerable progresses have been made by HPS, some critical issues need to be further addressed. These include 1) severe SWCNTs oxidation at high sintering temperature of 1500 °C, 2) low sintering density of 92 %, and 3) large amount of SWCNTs pull out due to weak interfacial bonding.

In order to fully densify the SWCNTs/Al_2O_3 composite ceramics without damaging the carbon nanotubes, Mukherjee *et al.* utilized a spark-plasma sintering (SPS) process.[9,10] 100% dense SWCNTs/Al_2O_3 composite ceramics were achieved at 1150 °C for 3 min with an applied pressure of 63 MPa and an electric pulse. A fracture toughness of 9.7 MPa $m^{1/2}$, nearly three times higher than that of pure nanocrystalline alumina, was achieved in the SPS sintered composite. Due to low-temperature sintering, it was found that the carbon nanotubes were not damaged during consolidation. Nonetheless, the SPS processing requires complex procedures and facilities that may not be viable for industrial large-scale applications.

Therefore, simple methods that can process high-strength carbon nanotube–alumina composites are essential for fabrication of large quantity structural materials. Furthermore, fundamental understanding of the interface structures between the carbon nanotubes and the alumina matrix is essential in further improving the mechanical properties. Based on our previous work,[11] we report experimental results of a systematic study on the development of surface nanostructures of single wall carbon nanotubes (SWCNTs) and alu-

a)Author to whom correspondence should be addressed. Electronic mail: shid@email.uc.edu. Tel.: 513 556 3100. FAX: 513 556 2569. Present address: University of Cincinnati, 493 Rhodes Hall, Cincinnati, Ohio 45221-0012

mina nanoparticles in the SWCNTs/Al_2O_3 composite by plasma polymerization. In particular, we show the pronounced effects of plasma surface functionalization on the thermal stability of SWCNTs and the mechanical behavior of the SWCNTs/Al_2O_3 composites. Transmission electron microscopy (TEM) results of surface functionalized SWCNTs and Al_2O_3 nanoparticles are presented. Experimental results on the sintering process, nanoparticle surface structures, dispersion behavior, and mechanical properties of the SWCNTs-Al_2O_3 composites are reported. The sintering mechanism related to the enhanced SWCNTs thermal stability is also discussed.

II. EXPERIMENTAL DETAILS

The SWCNTs/Al_2O_3 composite powders were prepared by the molecular level mixing with well-dispersed SWCNTs in the Al_2O_3 matrix.[11] The SWCNTs were provided by HELIX, having dimensions of 1.3 nm in diameter and 0.5–3 μm in length. The Al_2O_3 nanoparticles with the average diameter of 47 nm were purchased from Nanophase. The Al_2O_3 powders and SWCNTs were mixed in an ethanol solution and dispersed with an ultrasonner. The SWCNTs/Al_2O_3 gel was dried at 80 °C for 24 h. The dried solid was grounded into a fine powder. The volume fraction of SWCNTs was controlled at 7 and 9 wt %.

The plasma reactor for thin film deposition on nanoparticles consists mainly of a radio frequency (rf) source, the glass vacuum chamber, and pressure gauge.[12–15] The powder of SWCNTs/Al_2O_3 mixture with appropriate portions SWCNTs was placed on the fluidized bed and stirred mechanically. As the powders were being fluidized, they were charged in the rf zone. Before the plasma treatment, the basic pressure was pumped down to less than 100 mTorr, and then the monomer vapors were introduced into the reactor chamber. Pyrrole was used as a monomer in this work. The monomer residuals were deposited on nanoparticles and plasma polymerized. The operating pressure was adjusted by the gas/monomer mass flow rate. During the plasma polymerization process, the input power was 45 W, and the system pressure was 150 mTorr. The plasma treatment time was 30 min per batch. Each batch contained 2 g of powder.

Before sintering, a low-temperature consolidation procedure was employed for achieving high green density. The composite powders were pressed at 120 MPa in a rectangular die ($25\times7\times3$ mm^3) in ambient atmosphere. Due to surface coated polymer thin film, the movement of the particles was less hindered by the surface irregularities resulting in much higher green density during packing.[16,17] The compacted nanoparticles were heated at 250 °C for 2 h. After low-temperature consolidation, the SWCNTs/Al_2O_3 composite was placed in a tube furnace and sintered at 1000 °C for 12 h in a flowing gas mixture of 5 vol % H_2 and 95 vol % N_2. Upon heating, the sample was held at 500 °C for 1 h for polymer burn out. The SWCNTs/Al_2O_3 composites were also consolidated by HPS at 1200 °C. For HPS, the SWCNTs/Al_2O_3 mixed powder was loaded into a graphite die and compacted into a solid sample using direct current induced hot-press (dc hot-press) technique. A pressure of 120 MPa was used at a temperature of 1200 °C and held for 2 min.

The surface and interface structures of nanoparticles and ceramic matrix were studied by using TEM (JEOL 2010F). The SWCNTs/Al_2O_3 nanocomposite powders were dispersed onto the holey-carbon film supported for TEM. Time-of-flight secondary ion mass spectroscopy (TOF-SIMS) experiments were carried out to study the plasma deposited surface films on both SWCNTs and alumina nanoparticles. The TOF-SIMS analyses were performed on an ION-TOF Model IV instrument. In TOF-SIMS analysis, a pulsed primary ion beam was used to desorb and ionize species from a sample surface. The resulting secondary ions were accelerated into a mass spectrometer, where they were mass analyzed by measuring their time-of-flight from the sample surface to the detector. For each primary ion pulse, a full mass spectrum was obtained by measuring the arrival times of the secondary ions at the detector and performing a simple time to mass conversion.

The values obtained for the load and strain were the averages taken from three HPS specimens tested. Fractures of the HPS SWCNTs/Al_2O_3 composites with varying loadings and coating conditions were conducted in flexure mode on an Instron universal testing machine (Model # 4505). Three-point-bend test setup with a loading span of 20 mm was used. Nominal test sample dimensions were 3 mm $\times$4 mm$\times$25 mm, respectively. The tests on the HPS consolidated SWCNTs-Al_2O_3 samples were conducted at laboratory ambient conditions at a cross-head speed of 0.5 mm/min. The values obtained for the load and strain were the averages taken from three specimens tested.

The elastic modulus and compressive strength were determined by using a mechanical characterization loading stage system (Ernest F. Fullam, Inc., NY), with a load cell and strain-gage acquisition system. The cross-head speed was fixed at 0.02 mm/min and the strain-gage acquisition system was used to measure the strain accurately during compression loading. The values obtained for the load and strain were also the averages taken from three tested specimens.

III. EXPERIMENTAL RESULTS AND DISCUSSION

Figure 1 shows the high resolution transmission electron microscopy (HRTEM) images of plasma coated Al_2O_3 nanoparticles and SWCNTs in a mixed powder form. As can be seen, an ultrathin film of pyrrole is uniformly deposited on the surfaces of both SWCNTs and Al_2O_3 nanoparticles [Figs. 1(a)–1(c)]. The thickness of the ultrathin film is approximately 3 nm [see Fig. 1(c)]. It should be noted that although these nanoparticles have different sizes, the film has the same thickness indicating a uniform distribution of active radicals in the plasma chamber. In Figs. 1(a) and 1(b), one can see that the flexible SWCNTs appear to be curved around the alumina nanoparticles forming a good network in the sample mixture.

To further study and confirm the surface deposited-pyrrole thin films on SWCNTs and Al_2O_3 nanoparticles,

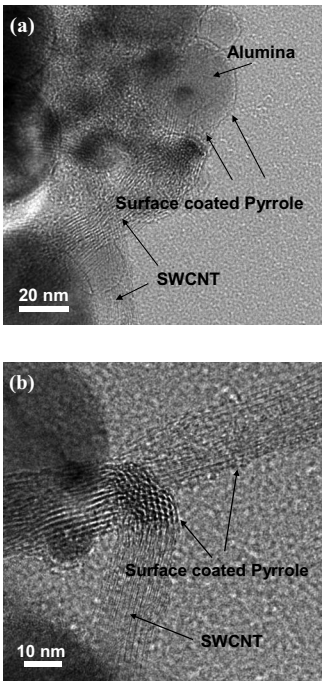

FIG. 1. (a) and (b) Bright-field TEM images of the plasma pyrrole coated SWCNTs and Al_2O_3 nanoparticles.

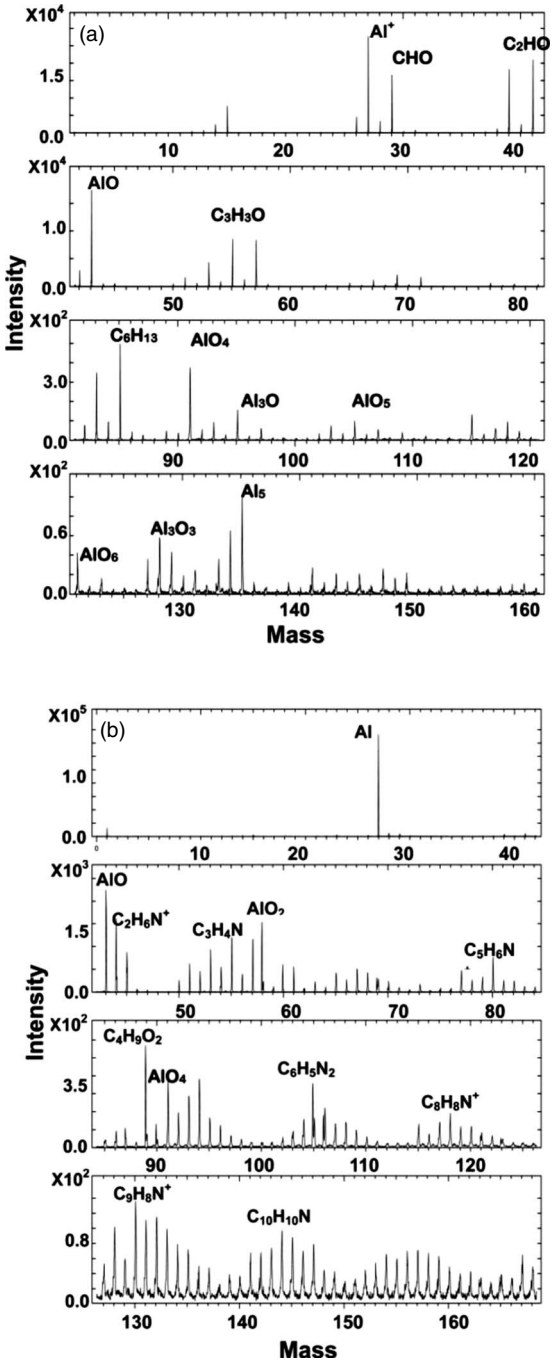

FIG. 2. (a) Positive TOF-SIMS spectra of uncoated and (b) positive TOF-SIMS spectra of pyrrole coated nanoparticles.

TOF-SIMS experiments were carried out. Figure 2 shows part of the TOF-SIMS positive spectra of plasma coated and uncoated SWCNTs/Al_2O_3 nanoparticles. Figure 2(a) shows the spectra of uncoated nanoparticles. In this figure, one can see the traces of $Al_xO_y^+$ groups and hydrolyzing of carbon on the sample surfaces. In Fig. 2(b), it can be seen that the coated SWCNTs/Al_2O_3 nanoparticles have strong nitrogen containing cluster $CxHyNz^+$ peaks. This indicates that the surfaces of nanoparticles are coated by pyrrole during plasma polymerization.[12] The repeated and continuous intensity peak in Fig. 2(b) is typical of plasma-polymerized clusters containing pyrrole. Even without sputtering, the surface is clean and free of siloxanes. The positive spectrum in Fig. 2(b) clearly shows a strong peak of Al^+ at +27 m/z which implies intensive sputtering of aluminum atoms from the particle surface during the initial phase of the plasma film deposition.[12] The appearance of the nitrogen containing clusters clearly indicates that the surfaces of SWCNTs-Al_2O_3 nanoparticles are well coated by plasma-polymerized pyrrole. These TOF-SIMS results are consistent with the HR-TEM images presented in Fig. 1.

Figure 3 shows the scanning electron microscopy (SEM) images of HPS consolidated SWCNTs/Al_2O_3 composites at 1200 °C. Figure 3(a) is the SEM image of the sample without plasma coating. In this figure, one can see that the sintered composite has a dense and uniform microstructure. In Fig. 3(b), the plasma coated counterpart shows a high density of SWCNTs, which are uniformly distributed in the sample matrix.

For comparison of sintering effects on density, the TEM images of SWCNTs/Al_2O_3 composites that were sintered at 1000 °C and HPS consolidated at 1200 °C are shown in Figs. 4(a) and 4(b), respectively. As can be clearly seen in Fig. 4(a), the low-temperature sintered sample has a porous microstructure, evidenced by many pores in the TEM image. Upon HPS at 1200 °C, however, the density is significantly increased as shown in Fig. 4(b).

The HRTEM image of a hot-press sintered sample with plasma coating is shown in Fig. 5. Consistent with the SEM microstructure shown in Fig. 3(b), the SWCNTs are well preserved and entangled within the Al_2O_3 grains. In particular, SWCNTs appear to form coherent and intimate interfaces with the Al_2O_3 grains. However, although the uncoated sample has a high density after HPS, SWCNTs are not found to be present in the matrix. Only individual Al_2O_3 grains can be seen in the TEM imag.[11]

Figures 6(a) and 6(b) show the stress versus strain

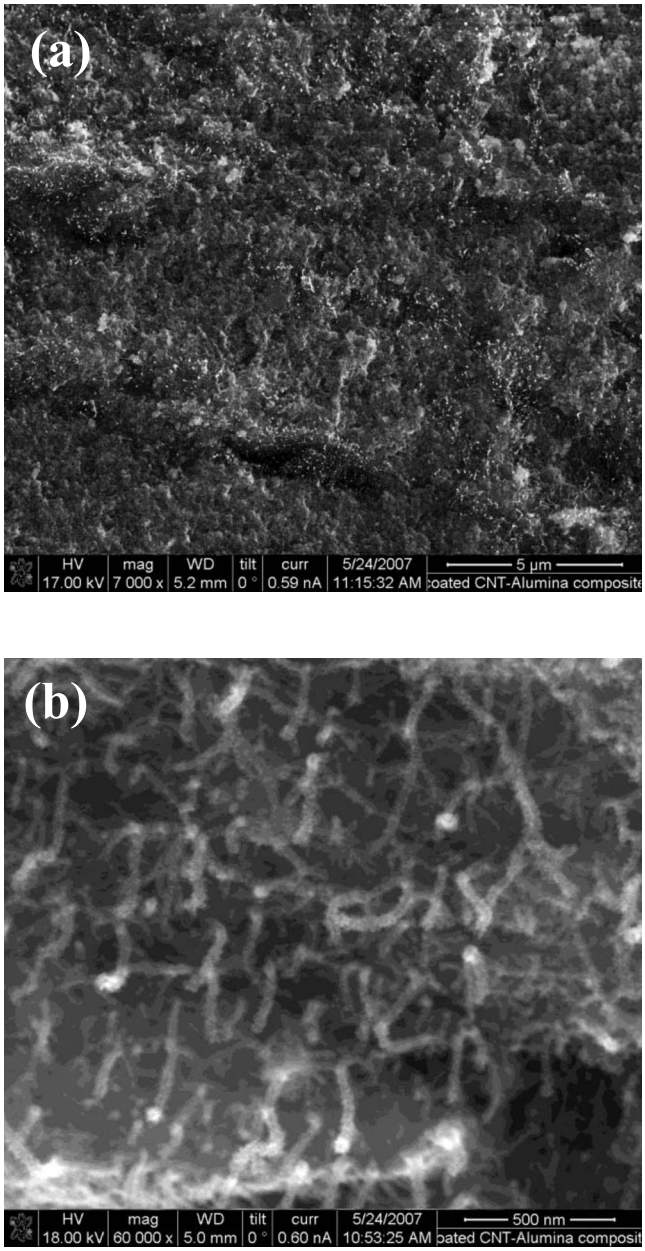

FIG. 3. SEM images showing (a) cross section of SWCNTs-Al_2O_3 composite without plasma coating, and (b) cross section of SWCNTs-Al_2O_3 composite with plasma coating.

curves of the HPS composite samples with 7 and 9 wt % SWCNTs, obtained in the compressive mode tests, respectively. As can be seen in this figure, the curve slopes exhibit clear differences between the plasma coated and uncoated samples. For both SWCNT loadings, the elastic moduli for the coated samples were significantly higher than those of the uncoated samples.

Figures 7(a) and 7(b) show the stress versus strain curves of the HPS composite samples with 7 and 9 wt % SWCNTs, obtained from the flexure mode, respectively. Consistent with the data shown in Fig. 6(a), the coated sample with 7 wt % SWCNTs exhibited higher flexural strength. The coated sample fractured at 164 MPa as compared to 143 MPa for the uncoated sample. However, for 9 wt % loading, the coated sample showed a lower strength

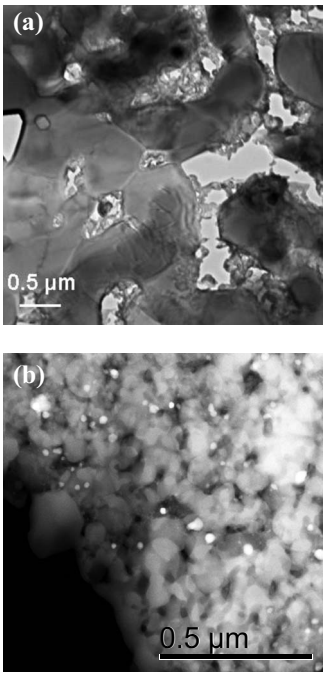

FIG. 4. Bright-field TEM images of the SWCNTs/Al_2O_3 composites, (a) sintered at 1000 °C under ambient pressure, and (b) hot-press sintered at 1200 °C.

(136 MPa) as compared to 166 MPa for the uncoated sample. The reduction in the flexural strength at 9 wt % loading has been attributed to the lower sample density as compared to the uncoated sample. Relative densities for the coated and uncoated 9 wt % loading samples were 90% and 94%, respectively. Effect of coating on the enhancement of mechanical properties in flexural tests is not as conclusive as demonstrated by the compressive tests. This is partly because the failure mechanism in the flexural mode is different from that in the compressive mode. It appears that the flexural tests are dominated by the effective sample porosity.

The stress-strain behaviors shown in Figs. 6 and 7 are consistent with the carbon nanotube surface structures observed in electron microscopy. There is a clear correlation between surface structures of SWCNTs and the mechanical behavior. For plasma coated samples, the SWCNTs in the composite matrix exhibit high thermal stability as evidenced in Figs. 1, 3, and 5. These SWCNTs form well connected networks at the interfaces of the alumina nanoparticles.

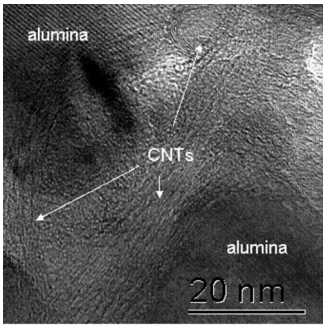

FIG. 5. Bright-field TEM image of the SWCNTs/Al_2O_3 composite, hot-press sintered at 1200 °C, showing well preserved SWCNTs entangled between the alumina grains.

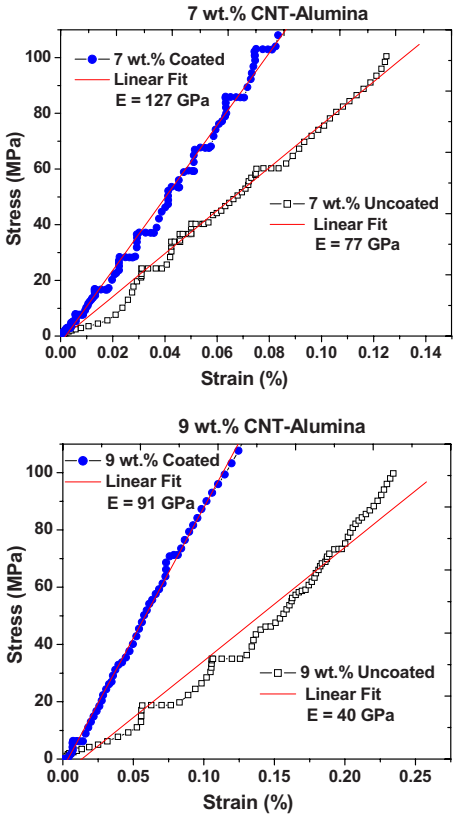

FIG. 6. (Color online) Stress-strain curves, obtained from the compressive mode, of the coated and uncoated SWCNTs/Al_2O_3 composites with 7 wt % SWCNTs.

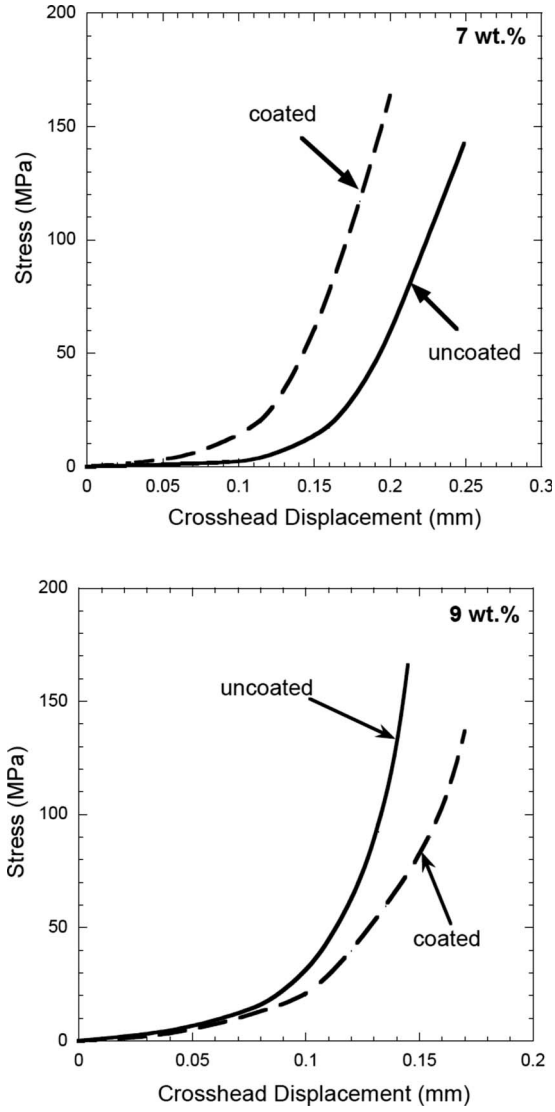

FIG. 7. Stress-strain curves, obtained from the flexure mode, of the coated and uncoated SWCNTs/Al_2O_3 composites with 7 wt % SWCNTs.

To further investigate the stability of SWCNTs in the composites, TEM experiments were carried out on low-temperature sintered (1000 °C) samples with and without plasma coating. Figure 8 shows the TEM images of low-temperature sintered composites. As shown in Figs. 8(a) and 8(b), for coated and uncoated samples, respectively, the SWCNTs exhibit distinctively different morphologies. In the coated sample, the SWCNTs remain structurally and morphologically unaltered with elongated nanotube features between the alumina grains. However, in the uncoated sample, the SWCNT bridges are mostly broken, forming clusters of carbon with the amorphous structures. Further TEM studies indicate that these SWCNTs are severely oxidized and significantly shortened as shown in Fig. 8(b).

Figures 8(c) and 8(d) show more detailed HRTEM structural features between the coated and uncoated samples, respectively. In Fig. 8(c), one can see well formed SWCNTs within the alumina structure in the coated sample. In contrast, however, Fig. 8(d) shows that most of SWCNTs have decomposed and disappeared in the sample matrix. Only residuals of amorphous carbon can be found in the alumina structures. Although the polymer films were assumed to be entirely burned out at the sintering temperature, their C-C bonds provided a protective layer that prevented SWCNTs from severe oxidation. From the SEM and TEM observations, there is clear evidence that the thermal stability of SWCNTs is significantly enhanced due to plasma coating. Thus, the plasma modified nanosurfaces and interfaces could play a critical role in the mechanical behaviors of SWCNTs-Al_2O_3 composites as evidenced in the compressive properties. Moreover, with plasma coating, the SWCNTs may withstand much higher sintering temperatures.

It should be noted that the enhanced mechanical properties are also likely associated with well dispersed SWCNTs in the matrix due to plasma coating. Although the quantitative determination of nanotube dispersion is currently underway, our previous studies on small angle light scattering and electron microscopy on surface treated carbon nanotubes showed significant enhancement of dispersion.[18] The SEM image in Fig. 3 also shows well dispersed SWCNTs network entangled in the matrix. As the nanoparticle surfaces are modified by plasma coating, the surface energy can be effectively lowered, resulting in improved dispersion.[18,19]

IV. CONCLUSIONS

A plasma polymerization method has been employed to deposit ultrathin pyrrole film on both SWCNTs and alumina nanoparticles for developing high-strength SWCNTs/Al_2O_3 nanocomposites. Both HRTEM and TOF-SIMS experimental

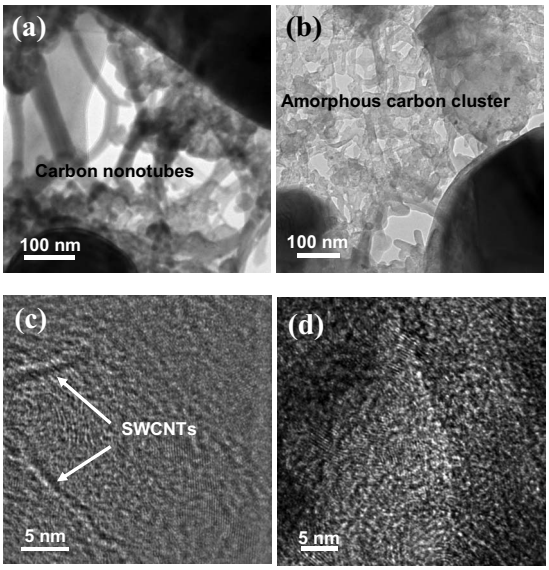

FIG. 8. Bright-field TEM images of the SWCNTs/Al_2O_3 composites sintered at 1000 °C under ambient pressure, showing (a) plasma coated SWCNTs with well preserved morphology and are connected to the alumina grains; (b) severely oxidized and shortened SWCNTs without plasma coating; (c) the SWCNTs embedded in the Al_2O_3 grain with well preserved crystal lattices due to protection of plasma coating, and (d) SWCNTs without coating are severely oxidized and reduced to the amorphous structure.

results have shown plasma deposited thin films on the carbon nanotubes and nanoparticles. The surface coating is not only ultrathin, on the order of a few nanometers, but also uniform. It has been found that the thermal stability of SWCNTs is enhanced due to plasma coating. This is well evidenced in TEM data that both morphology and crystal integrity of SWCNTS are preserved in the samples sintered up to 1200 °C. As a result of enhanced SWCNTs' thermal stability, the compressive mechanical properties of the composites are significantly improved. However, in flexural mode, fracture strengths for the coated and uncoated samples are somewhat similar. It is concluded in this study that the coated thin film provides an effective buffer layer on the SWCNTs, preventing them from severe oxidation at the sintering temperature. The plasma surface modification could also contribute to enhanced dispersion of SWCNTs as observed in the SEM study. These combined effects lead to an optimum surface structure, responsible for the enhanced mechanical properties.

ACKNOWLEDGMENTS

The authors are grateful to Chemat Technologies for the support under a U.S. Air Force SBIR grant. The TEM analyses were conducted at the Electron Microbeam analysis Laboratory at the University of Michigan and support supported by the Office of Basic Energy Sciences of the U.S. Department of Energy through Grant No. DE-FG02-97ER45656.

[1]P. M. Ajayan and O. Z. Zhou, in *Carbon Nanotubes*, edited by M. S. Dresselhaus and Ph. Avouris (Springer, Berlin, 2001).
[2]P. M. Ajayan, Chem. Rev. (Washington, D.C.) **99**, 1787 (1999).
[3]S. Iijima, Nature (London) **354**, 56 (1991).
[4]A. Peigney, Ch. Laurent, F. Dobigeon, and A. J. Rousset, Mater. Res. **12**, 613 (1997).
[5]E. Flahaut, A. Peigney, Ch. Laurent, Ch. Marliere, F. Chastel, and A. Rousset, Acta Mater. **48**, 3803 (2000).
[6]X. Devaux, Ch. Laurent, M. Brieu, and A. Rousset, in *Composite Materials*, edited by A. T. Di Benedetto, L. Nicolais, and R. Watanabe (Elsevier, New York, 1992), p. 209.
[7]Ch. Laurent, A. Peigney, O. Dumortier, and A. Rousset, J. Eur. Ceram. Soc. **18**, 2005 (1998).
[8]A. Peigney, Ch. Laurent, E. Flahaut, and A. Rousset, Ceram. Int. **26**, 677 (2000).
[9]G. Zhan, J. Kuntz, J. Wan, and A. K. Mukherjee, Nat. Mater. **2**, 38 (2003).
[10]R. Riedel, *Handbook of Ceramic Hard Materials* (Wiley, New York, 2000), p. 649.
[11]Y. Guo, D. Shi, J. Lian, H. S. Cho, Y. Song, J. Abot, Z. Ren, B. Poudel, L. Wang, and R. C. Ewing, Appl. Phys. Lett. **91**, 261903 (2007).
[12]D. Shi, S. X. Wang, W. J. van Ooij, L. M. Wang, J. Zhao, and Z. Yu, J. Mater. Res. **17**, 981 (2002).
[13]D. Shi, P. He, J. Lian, L. M. Wang, and W. J. van Ooij, J. Mater. Res. **17**, 2555 (2002).
[14]D. Shi, S. X. Wang, W. J. van Ooij, L. M. Wang, J. Zhao, and Z. Yu, Appl. Phys. Lett. **78**, 1243 (2001).
[15]D. Shi, J. Lian, P. He, L. Wang, W. J. Van Ooij, M. Schulz, Y. Liu, and D. B. Mast, Appl. Phys. Lett. **81**, 5216 (2002).
[16]D. R. Dinger and J. E. Funk, Fine Particle Society, 13th Annual Meeting, Chicago, 1982 (unpublished).
[17]J. Zheng, P. F. Johnson, and J. S. Reed, J. Am. Ceram. Soc. **73**, 1392 (1990).
[18]J. Zhao, D. W. Schaefer, D. Shi, J. Lian, J. Brown, G. Beaucage, L. Wang, and R. C. Ewing, J. Phys. Chem. B **109**, 23351 (2005).
[19]D. Shi, J. Lian, P. He, L. Wang, M. Schultz, and D. B. Mast, Appl. Phys. Lett. **83**, 5301 (2003).